

shown in Table 4, which arise from the fact that the model does not quite have  $R\bar{3}$  symmetry.

So far we have considered only the anions of the structure, because it is these which are displaced significantly from ideal fluorite sites. The cations suffer only minor displacements from the ideal f.c.c. positions. However, only those cation sites in the models which can, to a good approximation, be centred within *regular* polyhedra (e.g. square antiprisms, cubes) can be calculated. Thus, for example, the coordinates of the 18(*f*) Zr site in  $\text{Na}_7\text{Zr}_6\text{F}_{31}$  are calculable, but not for the 18(*f*) Na(1) site. Comparative data for  $\text{Na}_7\text{Zr}_6\text{F}_{31}$  are shown in Table 5.

Overall, then, for the three structures discussed, the calculations are in good agreement with observations, and we consider the polyhedral models to be good approximations to the real structures. In a subsequent paper we shall show how such calculations on a polyhedral model of a *postulated* structure have

been used, with X-ray powder data, as the starting point of a successful refinement.

We thank Dr H. J. Rossell and Professor B. Abrahamson for much helpful discussion.

We also acknowledge the provision of financial assistance by the Australian Research Grants Scheme.

#### References

- ALÉONARD, S., LE FUR, Y., PONTONNIER, L., GORIUS, M. F. & ROUX, M. T. (1978). *Ann. Chim.* **3**, 417-427.  
 BEVAN, D. J. M., GREIS, O. & STRÄHLE, J. (1980). *Acta Cryst.* **A36**, 889-890.  
 BEVAN, D. J. M., STRÄHLE, J. & GREIS, O. (1982). *J. Solid State Chem.* **44**, 75-81.  
 BURNS, J. H., ELLISON, R. D. & LEVY, H. A. (1968). *Acta Cryst.* **B24**, 230-237.  
 PIERCE, J. W. & HONG, H. Y. P. (1973). *Proceedings of the Tenth Rare-Earth Research Conference*, edited by C. J. KEVANE, pp. 527-537. US Atomic Energy Commission, Technical Information Center.

*Acta Cryst.* (1986). **B42**, 58-61

## Textures in Natural Pyrolusite, $\beta\text{-MnO}_2$ , Examined by 1 MV HRTEM

BY N. YAMADA AND M. OHMASA

*Institute of Materials Science, University of Tsukuba, Ibaraki 305, Japan*

AND S. HORIUCHI

*National Institute for Research in Inorganic Materials, Ibaraki 305, Japan*

(Received 1 July 1985; accepted 23 August 1985)

### Abstract

Textures in natural pyrolusite have been studied by 1 MV high-resolution transmission electron microscopy (HRTEM). The structure is mainly of the rutile type with many lamellae of a different structure. Most of the lamellae, being parallel to each other, are perpendicular to one of the tetragonal *a* axes of the pyrolusite and are separated by about 9 nm. Their structure was inferred to be similar to that of ramsdellite. There are many holes located along the lamellae. The cross section of some holes is rhombic and their edges are almost parallel to  $\langle 110 \rangle$ ; they vary in size from ten to several hundred  $\text{nm}^2$ . The holes must be produced in the process of the phase transformation of manganite into pyrolusite.

### Introduction

The structure unit in manganese oxides and hydroxide oxides is an  $\text{MnO}_6$  octahedron, which shares opposite edges with adjoining octahedra to

form an infinite chain. The period of the chain is 0.28 nm. Double or triple chains are formed when two or three parallel chains are combined with each other by sharing edges of the constituent octahedra. Many varieties of framework structures have so far been found for manganese oxides which are built of single or multiple chains by sharing their corners (Wells, 1975).

There are three reasons why the study of the phase and structure relation among these compounds is difficult: (i) many polymorphs with different combinations of chains have been found in these compounds, but the stability relation among them is still not clear; (ii) various kinds of cations can be easily accommodated in the interstices of the framework and give a complex formula; in this case some of the  $\text{Mn}^{4+}$  in the framework are replaced by  $\text{Mn}^{3+}$  or other cations with smaller charges; and (iii) many of these compounds are often found or synthesized as brittle, poorly crystallized materials. (iii) is the principal reason why these materials have not yet been fully characterized crystallographically. Consequently,

many problems remain unsettled, though these materials are important for industrial use as catalysts or electrolyte materials in dry batteries.

Since the resolving power of electron microscopes has been highly improved in recent years, it is now possible to observe the structural irregularity in crystals on an atomic scale and the physical properties of materials can be discussed directly in relation to defect structures or microtextures (Turner & Buseck, 1983). We have, therefore, used this approach to examine the problems of manganese oxides and hydroxide oxides.

Recently we found that single crystals of pyrolusite from various localities display distinct diffuse streaks in X-ray diffraction patterns. These streaks reveal that the crystals include structural irregularity. The present studies have been carried out to elucidate the irregularity by electron microscopy.

### Experimental

Two specimens of natural pyrolusite in the mineral collection of the Museum in the Geological Survey of Japan were available for the present experiment: one from Australia (Woody-Woody mine, cat. No. GSJ M 17980) and the other from Malaysia (cat. No. GSJ M 17981). These were examined by X-ray diffraction. The symmetry of both specimens was determined to be tetragonal ( $P4_2/mnm$ ) with lattice parameters  $a = 4.400$  (2) and  $2.871$  (2) Å. However, they all exhibited two systems of diffuse streaks along one of the  $a^*$  axes of the reciprocal lattice.

Some crystals from both specimens were selected for observation by HRTEM. They are euhedral and show (elongated along the  $c$  axis) prismatic forms with average dimensions  $0.5 \times 0.5 \times 1.0$  mm. The elongation is more prominent in the crystals from Malaysia than in those from Woody-Woody mine.

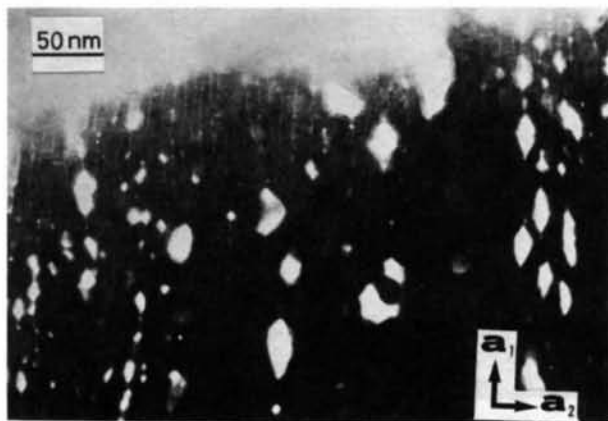


Fig. 1. Low-magnification image of pyrolusite from Woody-Woody mine. The incident electron beam is parallel to the  $c$  axis of  $\beta$ - $MnO_2$ .

Small blocks of the crystals were sliced by a razor blade and the thin fragments obtained were observed in a 1 MV electron microscope (H-1250 type). The direct magnification was  $2.5 \times 10^5$  and the incident beam was parallel to the  $c$  axis (Yamada, Ohmasa & Horiuchi, 1984).

### Results and discussion

A transmission electron micrograph of the pyrolusite from Woody-Woody mine indicates two characteristics: one is many holes scattered within the whole crystal and the other is lamellae parallel to one of the  $a$  axes of the tetragonal cell (Fig. 1). The interval between adjoining lamellae is roughly equal. The holes are located along the lamellae or along their extension. Similar features are also found on electron micrographs of the sample from Malaysia (Fig. 4a).

Fig. 2 is a magnified image of a thin edge area of the specimen of Fig. 1. Most of it consists of the structure in which two sets of lattice fringes of width 0.44 nm cross at right angles. The intervals of the fringes correspond to the cell parameters of  $\beta$ - $MnO_2$ . Similar fringes are also observed in micrographs of the specimen from Malaysia. A HRTEM image of a thin edge area in a Malaysian crystal is illustrated in Fig. 3 together with a computer-simulated image. Since these two coincide well, the structures of both specimens were confirmed to be of  $\beta$ - $MnO_2$  with the rutile-type structure.

Many lamellae are also observed in Fig. 2 and the width of the lattice fringes in the lamellae is different from that in  $\beta$ - $MnO_2$ . Since the width in the lamellae is about 0.9 nm and this value coincides with the length  $b$  of ramsdellite (Byström, 1949), the structure seems identical to that of ramsdellite. The interval between the lamellae fluctuates at random and the mean value is about 9 nm in the sample from Woody-

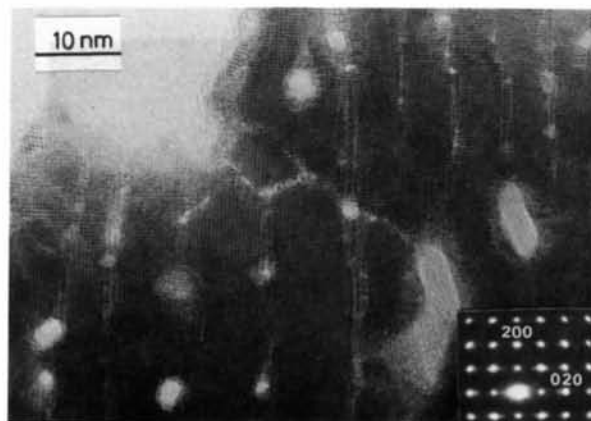


Fig. 2. HRTEM image and electron diffraction pattern of the same crystal shown in Fig. 1.

Woody mine and about 8 nm in that from Malaysia. The selected-area diffraction pattern is inserted in Fig. 2, in which diffuse streaks are observed in the direction parallel to the  $a_2^*$  axis. Their origin may be attributed to the random fluctuation mentioned above. These diffuse streaks correspond to one of the two systems of the diffuse streaks found by X-ray diffraction and the details of the two systems will be discussed elsewhere.

A phase transformation from  $\beta$ - $\text{MnO}_2$  to  $\gamma$ - $\text{Mn}_2\text{O}_3$  or  $\text{Mn}_3\text{O}_4$  (hausmannite) occurs when the specimen is irradiated by the incident beam with much higher intensity. Fig. 4(a) indicates the state before the transformation. In Fig. 4(b), the lamellae have completely disappeared and part of the  $\beta$ - $\text{MnO}_2$  has transformed into  $\gamma$ - $\text{Mn}_2\text{O}_3$  or  $\text{Mn}_3\text{O}_4$ . Terayama & Ikeda (1981) and Jerez & Alario (1982) have reported that the transformation takes place when  $\beta$ - $\text{MnO}_2$  is heated. Therefore, the present transformation is probably caused by a temperature rise during the strong illumination by the electron beam.

The form of some of the holes in Fig. 1 is rhombus or rhomboid and their edges are nearly parallel to  $\langle 110 \rangle$  of  $\beta$ - $\text{MnO}_2$ . The area of each hole was measured in Fig. 1 and the mean area of the holes is  $110 \text{ nm}^2$ . The ratio of the total area of the holes to the area of the crystal plus holes is about 12%. Pyrolusite crystals often occur as euhedral crystals, but these are in most cases pseudomorphs after manganite ( $\gamma$ - $\text{MnOOH}$ ). This suggests that most euhedral pyrolusites are products of the phase transformation from manganite (Ford, 1957). Since the molar volume of  $\gamma$ - $\text{MnOOH}$  is larger than that of  $\beta$ - $\text{MnO}_2$  by 17%, the volume of the material contracts in the process of phase transformation by losing H. The contribution of the contraction to the total area of the holes was then estimated from the difference of the molar volumes on the assumption that the three dimensions of the holes are equal. The value obtained was 11%. This

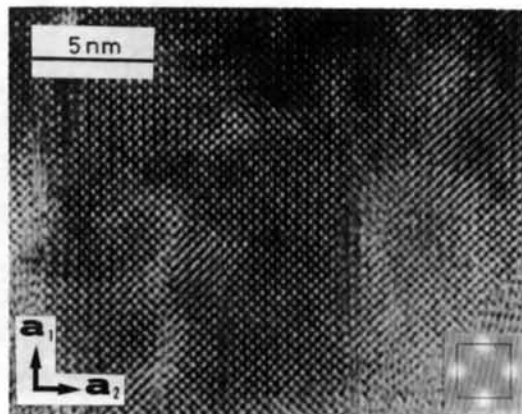


Fig. 3. HRTEM image of pyrolusite from Malaysia and the corresponding computer-simulated image.

value is in good agreement with that, 12%, estimated from Fig. 1. Consequently, the holes observed in the electron micrographs must be produced in the process of the phase transformation. The formation of the lamellae may be strongly related to that of the holes, but the relation between them is still not clear.

Manganese dioxides usually have a large specific surface area and this feature is one of the factors which improves the activities of catalysts. Since the present specimens have many holes, their specific surface area must be very large and may serve to provide good catalytic activity.

The authors thank Dr M. Bunno, Geological Survey of Japan, for providing the specimens, and Dr K. Wada and Mr Y. Kitami, National Institute for Research in Inorganic Materials, for their help in the experiments. They are also grateful to Professor T. Fujii for a critical reading of the manuscript. This work was partly supported by a Grant-in-Aid for Scientific Research from the Ministry of Education of Japan.



(a)



(b)

Fig. 4. (a) HRTEM image and electron diffraction pattern of pyrolusite from Malaysia. (b) The same area as (a) after strong illumination by the electron beam.

## References

- BYSTRÖM, A. M. (1949). *Acta Chem. Scand.* **3**, 163–173.  
 FORD, W. E. (1957). *A Textbook of Mineralogy*. New York: John Wiley.  
 JEREZ, A. & ALARIO, M. A. (1982). *Thermochim. Acta*, **58**, 333–339.  
 TERAYAMA, K. & IKEDA, M. (1981). *J. Jpn Inst. Met.* **45**, 901–908.  
 TURNER, S. & BUSECK, R. (1983). *Nature (London)*, **304**, 143–146.  
 WELLS, A. F. (1975). *Structural Inorganic Chemistry*, 4th ed. Oxford: Clarendon Press.  
 YAMADA, N., OHMASA, M. & HORIUCHI, S. (1984). *3rd Asia-Pacific Conference and Workshop on Electron Microscopy*, pp. 192–193.

*Acta Cryst.* (1986). **B42**, 61–68

## Defect Structure Dependence on Composition in Lithium Niobate

BY S. C. ABRAHAMS AND P. MARSH

*AT&T Bell Laboratories, Murray Hill, New Jersey 07974, USA*

(Received 11 June 1985; accepted 4 September 1985)

### Abstract

The lattice constants of stoichiometric  $\text{LiNbO}_3$  and congruent [ $\text{Li}_2\text{O}:\text{Nb}_2\text{O}_5 = 48.45:51.55$ ] composition lithium niobate at 298 K are  $a = 5.14739$  (8),  $c = 13.85614$  (9) [ $a = 5.15052$  (6),  $c = 13.86496$  (3)] Å for Cr  $K\alpha_1 = 2.28970$  Å in space group  $R3c$  with  $V = 317.941$  [318.513] Å<sup>3</sup>,  $M_r = 147.846$  [148.551],  $D_m = 4.635$  (5) [4.648 (5)],  $D_x = 4.6327$  [4.646] Mg m<sup>-3</sup> for  $Z = 6$ ,  $F(000) = 408$  [409.89],  $\mu = 5.116$  [5.165] mm<sup>-1</sup>. All reflections in the reciprocal-lattice spheres of both compositions with  $(\sin \theta)/\lambda \leq 1.1$  Å<sup>-1</sup> were measured, with 746 [769] symmetry independent  $F_m^2 > 3\sigma F_m^2$ . Final  $R(F) = 0.0117$  [0.0121]. No atomic disorder was detected in stoichiometric  $\text{LiNbO}_3$  but 6% Li is missing from all Li sites in the congruent composition. Each missing  $\text{Li}^+$  ion is replaced by an  $\text{Nb}^{5+}$  ion, with compensating vacancies at the Nb site maintaining charge neutrality, as given by the formula  $[\text{Li}_{1-5x}\text{Nb}_{5x}]\text{Nb}_{1-4x}\text{O}_3$  with  $x = 0.0118$  (7) in the congruent composition. The stability range of the nonstoichiometric composition corresponds to  $0 \leq x \leq 0.02$ . Lithium vapor-phase equilibration of congruent material at 1373 K or higher temperature is postulated to involve: Nb-ion migration from Li to Nb sites by about  $3.1$  Å through an octahedral face of O atoms followed by Li atoms filling the resulting vacancies; an exchange between the remaining Nb at Li sites with other Li atoms; and formation of an oriented overgrowth of additional unit cells. The Nb-ion displacement of  $0.2768$  [0.2701] Å along the polar axis from the mid-position between O-atom planes allows the Curie temperature to be predicted as 1532 [1459] K; the experimental Curie temperature is 1471 [1402] K. Anharmonic thermal vibrations were detected only in the congruent composition.

### Introduction

The properties and applications of lithium niobate have been widely studied, resulting in the publication of more than three thousand papers on this material since 1967 and over one thousand since 1980. A detailed review of the physics and chemistry of lithium niobate has been given by Räuber (1978), whose two hundred or more references provide ready access to the literature. The high level of interest in lithium niobate, originating in its combination of useful dielectric, elastic and optoelectronic properties together with the ready growth of large high-quality single crystals from the melt, has recently increased even further as its electrooptic-device use has led to optical switching speeds as fast as 50 ps. In consequence, high-speed switches, modulators, waveguide arrays, multiplexers, filters and polarization converters have been built based on lithium niobate. Stoichiometric lithium niobate melts incongruently. The congruent melting temperature of 1513 K corresponds to the formula  $\text{Li}_{0.946}\text{NbO}_{2.973}$  (Carruthers, Peterson, Grasso & Bridenbaugh, 1971). Many physical properties are dependent, some with considerable sensitivity, on the Li:Nb ratio as well as on the precise oxidation state of the crystal. An easily measured and strongly composition-dependent property is the Curie temperature of this ferroelectric crystal. Gallagher & O'Bryan (1985) report  $T_c = 1471$  (2) K for  $\text{LiNbO}_3$  and 1402 (2) K for  $\text{Li}_{0.946}\text{NbO}_{2.973}$ , with a range of  $\pm 0.007$  Li from this nominal congruent composition. A smaller, but still significant, dependence on composition has been found both for the lattice constants and the density by Lerner, Legras & Dumas (1968). Measurements made on crystals with composition-dependent properties clearly have larger variances than those estimated only from the experimental